

Variable Crystallinity Polyethylene Nanoparticles

Sze-Man Yu and Stefan Mecking*

Chair of Chemical Materials Science, Department of Chemistry, University of Konstanz, Universitätsstr. 10, D-78457 Konstanz, Germany

Received February 17, 2009; Revised Manuscript Received March 30, 2009

ABSTRACT: Water-soluble complexes based on enolatoimine ligands bearing electron-withdrawing trifluoromethyl groups [κ^2 -*N,O*-{2,6- $R_2C_6H_3N=C(H)C(COCF_3)=C(OCF_3)NiMe(L)$] (**1a**, $R = 3,5-(CF_3)_2C_6H_3$, $L = Me(OCH_2CH_2)_nNH_2$; **1b**, $R = 3,5-(CF_3)_2C_6H_3$, $L = TPPDS$; **2b**, $R = ^iPr$, $L = TPPDS$; **2c**, $R = ^iPr$, $L = TPPTS$ with $TPPDS = PhP(p-C_6H_4SO_3Na)_2$ and $TPPTS = P(m-C_6H_4SO_3Na)_3$) were prepared. These complexes polymerize ethylene to very small (10–30 nm) semicrystalline particles of high molecular weight (up to $M_w 1.6 \times 10^6$ g mol⁻¹) polymer with a degree of branching (7–63 branches per 1000 C atoms) and thus crystallinity (≤ 25 –50%) and melt transition temperatures ($T_m = 75$ –129 °C) variable over a large range, depending on the substituents of the *N*-aryl moiety (2,6- $R_2C_6H_3$), and the polymerization temperature. The catalysts are stable for hours under polymerization conditions (50 °C) in the highly disperse aqueous system.

Introduction

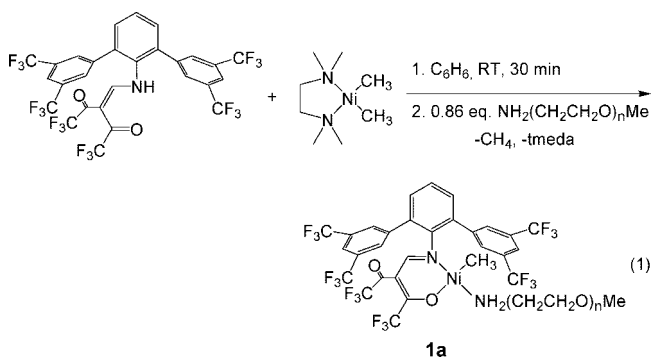
Polymer nanoparticles are of broad academic and industrial interest.¹ Examples of specific topics of interest are the introduction and transport of guest molecules such as poorly soluble drugs, carriers in aqueous multiphase catalysis, or homogeneous incorporation of functional molecules into solid materials.² In many cases, nanoscale entities of <30 nm size are desirable. Also, the presence of the particles as aqueous dispersions is required. While studies of particles in this size regime originating from free-radical microemulsion polymerization³ have mostly been concerned with amorphous polymers, such small semicrystalline particles are also attractive. They can, for example, contribute to fundamental understanding of crystallization in confinement, crystallinity can be a source of anisotropy, and such particles can serve as crystalline mesoscopic building blocks for ultrathin films.^{4,5} Polyethylene is of interest in this context as it is the simplest organic polymer in terms of molecular structure, and its crystallization and structure in the bulk have been investigated more intensely than for any other polymer.⁶ As a saturated hydrocarbon, polyethylene is apolar and hydrophobic and inert toward hydrolysis or other decomposition reactions. Single lamella nanoscale (6 nm lamella thickness, ca. 25 nm pseudodiameter) crystals of high molecular weight linear polyethylene are accessible by catalytic polymerization with water-soluble Ni(II) salicylaldiminato complexes.⁷ However, in terms of the aforementioned issues, a viable route to nanoparticles in this size regime with broadly variable crystallinity appears desirable.

Results and Discussion

Synthesis and Characterization of Catalyst Precursors. Polymerization of ethylene with aqueous solutions of in situ prepared Ni(II)- κ^2 -*P,O*-phosphinophenolato complexes affords ca. 20 nm particles of linear polyethylene. These ill-defined catalysts are stable under polymerization conditions (for >7 h). Because of a relatively high propensity for β -hydride elimination of the catalyst, the polymer formed possesses limited molecular weight (typically M_w ca. 10^4 g mol⁻¹).⁸ High molecular weight linear polyethylene nanocrystals are accessible with water-soluble κ^2 -*N,O*-salicylaldiminato-Ni(II) methyl complexes as well-defined precursors.^{5b,9} For lipophilic versions of this catalyst type, it has been demonstrated that the degree of branching and thus crystallinity of the polymers formed can be varied over a wide range by appropriate choice of remote

substituents of the salicylaldiminato ligand, as demonstrated in nonaqueous systems.¹⁰ These catalysts can be stable for hours in nonaqueous polymerizations and also in aqueous polymerizations employing miniemulsions of lipophilic catalyst precursors (affording typically particles of 100 to several 100 nm average size).¹⁰ However, the stability and lifetime of these catalysts in the highly disperse aqueous systems obtained with the aforementioned water-soluble catalyst precursors are limited, typically after ca. 30 min polymerization has ceased.^{9,11} For this reason, an alternative approach was sought to the desired variable crystallinity nanoparticles. An increased electrophilicity of the Ni center, brought about by electron-withdrawing substituents in the bidentate *N,O*- or *P,O*-coordinating ligand, substantially increases the polymerization rates.¹² Enolatoimine Ni(II) phenyl or methyl complexes, respectively [κ^2 -*N,O*-{ArN=CH-C(COCF₃)=C(CF₃)O}NiR(L)] with strongly electron-withdrawing trifluoromethyl and trifluoroacetyl groups are very active for the synthesis of high molecular weight polyethylene.^{12b,c} Polymerizations with such electron-deficient systems can be carried out in aqueous emulsions to afford stable polyethylene dispersions. Surprisingly, in view of the electron-deficient nature of the metal sites, even at a high temperature of 70 °C catalyst stability is sufficient for the polymerization to continue for hours.^{12c} Therefore, water-soluble enolatoimine complexes appeared of interest for polyethylene nanoparticle synthesis.

[(tmeda)Ni(CH₃)₂] was employed as a Ni(II) source (tmeda = *N,N,N',N'*-tetramethylethylenediamine). Reaction with a ketoenamine results in expulsion of one Ni–Me group as methane to afford [(NO)NiMe(tmeda)] as an intermediate, which reacts immediately with Me(OCH₂CH₂)_nNH₂ upon addition of the latter (eq 1).



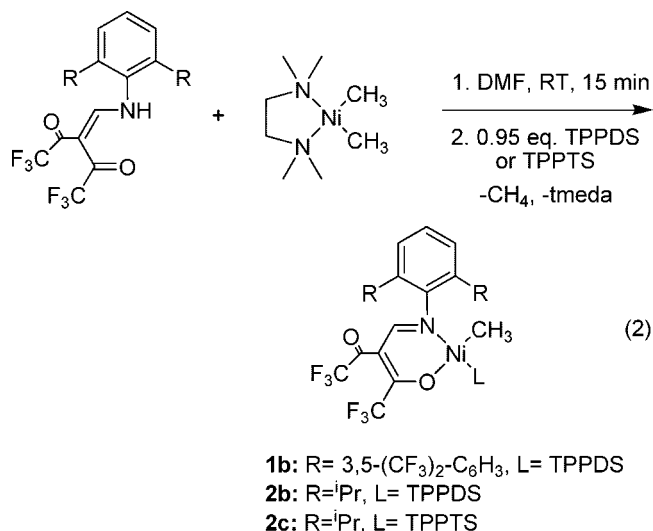
* Corresponding author. E-mail: stefan.mecking@uni-konstanz.de.

Table 1. Polymerization under Aqueous Conditions^a

entry	catalyst precursor	cat. [10 ⁻⁶ mol]	time [h]	temp [°C]	TON [mol (C ₂ H ₄) mol (Ni) ⁻¹]	polymer yield [g]	M_w^b [10 ³ g mol ⁻¹]	M_w/M_n^b	crystallinity ^c [%]	T_m^c [°C]	particle size ^d [nm]
1	1a	8	0.5	50	3220	0.72	170	5.4 ^f	42	105/119	105
2	1a	10	0.5	15	890	0.25	180	2.8 ^f	48	123	60
3	1a	10	0.5	70	1180	0.33	40	3.7	38	95/110	144
4	1a	10	0.5	50	2540	0.71	130	3.0 ^f	43	104/117	150
5	1a	10	0.5	40	3760	1.05	840	6.1 ^f	44	126	26
6	1a	10	5	30	5360	1.50	1600	6.4 ^f	45	129	29
7	1b	8	1	40	890	0.2	200	16.7 ^f	50	123	15
8	1b	50	16	40	6000	8.4	110	5.1 ^f	43	104	101
9	2b	10	1	40	1710	0.48	20	2.4	35	83/99	12
10	2b	10	0.5	50	1210	0.34	20	2.4	34	77/99	12
11	2b	10	8	50	6070	1.70	20	2.5	33	75/95	14
12 ^e	2b	100	10	50	2390	6.70	10	3.2	≤25	n.d.	18
13	2c	10	0.5	50	1430	0.40	20	2.5	36	76/94	11
14	2c	10	0.5	60	430	0.12	10	3.0	≤25	76	11

^a Reaction conditions: 100 mL of degassed water, 750 mg of SDS, 40 bar of ethylene, polymer obtained as latex. ^b Determined by GPC vs linear PE standards. ^c Determined by DSC on bulk polymer. ^d Number-average particle size determined by DLS. ^e 1.25 g of SDS. ^f Bimodal distribution.

1a was characterized by ¹H, ¹³C, and ¹⁹F NMR spectroscopy. The ¹³C NMR resonances were fully assigned by ¹H, ¹H gCOSY, heteronuclear ¹H, ¹³C 2D NMR, and ¹H, ¹³C 2D long-range-coupling NMR spectroscopy. The characteristic NH signal (δ = 11.44 ppm) of the ketoenamine is absent in **1a**. The N–CH= proton gives rise to a singlet at δ = 7.49 ppm in **1a** vs a doublet in the free ketoenamine (δ = 6.83 ppm). In ¹H NMR and ¹³C NMR spectra of complex **1a**, only a single Ni–Me resonance is observed. This shows that only one isomer with respect to the stereochemistry at the square-planar Ni(II) center is formed. In analogy to solid state structures of similar complexes,^{10a,b,12b,13} the Ni–Me group is very likely bound in cis position to the imine moiety. For the CF₃-substituted aryl rings, only one ¹³C NMR resonance is observed for the CF₃ groups and the *o*- and *m*- carbon atoms, respectively. In accordance, also only a single ¹⁹F resonance is observed for the CF₃ group of the terphenyl moiety. This indicates a rapid rotation of the CF₃-substituted aryl rings about the bond to the central N-bound aryl ring. This parallels the dynamics observed for the analogous pyridine complex. Overall, the resonances originating from the enolatoimine ligand (NO) in **1a** are similar to the related compound [(NO)NiMe(pyridine)].^{12c}



The sulfonated phosphine complexes **1b**, **2b**, and **2c** were prepared from [(tmeda)Ni(CH₃)₂], ketoenamine ligand, and TPPDS or TPPTS, respectively, in DMF as a solvent (eq 2; TPPDS = PhP(*p*-C₆H₄SO₃Na)₂; TPPTS = P(*m*-C₆H₄SO₃Na)₃).

The phosphine complexes contain one to two molecules of DMF, which are presumably coordinated to the sodium counterions of TPPDS and TPPTS, respectively. In **2b** and **2c**, the

Ni–Me protons resonate at δ = –1.24 and –1.20 ppm, respectively. A P–H coupling is not observed; however, the ¹³C NMR resonance of the Ni–Me moiety displays coupling (²*J*_{CP} = 24 Hz) to the phosphorus atom of coordinated TPPTS (**2c**), as expected. For **2b**, a broad signal is observed for the Ni–Me protons, which is likely due to an unresolved ³*J*_{PH} coupling.

Synthesis of Aqueous Dispersions. Exposure of an aqueous SDS solution of the water-soluble Ni complexes to ethylene in a pressure reactor afforded stable dispersions (Table 1). This demonstrates that despite the strongly electron-withdrawing nature of the enolatoimine ligands in the catalysts studied, catalyst stability toward water is sufficient to carry out polymerizations starting from an entirely aqueous system.

Productivities on the order of 10⁴ mol (ethylene) mol (Ni)⁻¹ were observed. These activities are comparable with known neutral κ^2 -*N,O*-salicylaldiminato-Ni(II) complexes. A study of the influence of reaction temperature showed that the catalyst formed from **1a** is most productive at 40 °C (Table 1, entries 2–5). With complex **2b** and **2c** as a catalyst precursor, highest activities were observed at 50 °C. A conspicuous difference in detail between enolatoimine- and salicylaldimine-based catalysts⁹ is that a high activity was observed for the latter system already at polymerization temperatures of 15 °C, but rapid decomposition occurred at 50 °C, whereas for the enolatoimine complexes subject to this study 40–50 °C is required for efficient polymerization. This may be due to a stronger coordination of the amine or phosphine, respectively, dissociation of which is a prerequisite for polymerization, due to the electron deficiency of the Ni(II) center, which results from the more strongly electron-withdrawing enolatoimine ligand.

Dispersions of very small nonaggregated crystalline particles were generally obtained. Only in some experiments at elevated temperatures and for higher final solids contents (entries 1, 3, 4, and 8), larger average particle sizes were determined by DLS, presumably due to weak aggregation of particles. In contrast to previously reported polymerization with water-soluble salicylaldiminato-Ni(II) complexes as catalyst precursors, the enolatoimine-substituted complexes are stable for hours under polymerization conditions, despite the equally high degree of dispersion of the reaction mixture obtained with these catalysts (entries 7 vs 8 and entries 10 vs 11). Consequently, a substantially higher solids content of polymer could be obtained. Dispersions of up to 8.4 wt % polymer solids content were prepared, without further optimization.

The microstructure of the polymers was studied by quantitative ¹³C NMR spectroscopy.¹⁴ In addition to methyl branches as the major branch type, ethyl and higher branches are observed. This branching pattern and degree of branching (vide

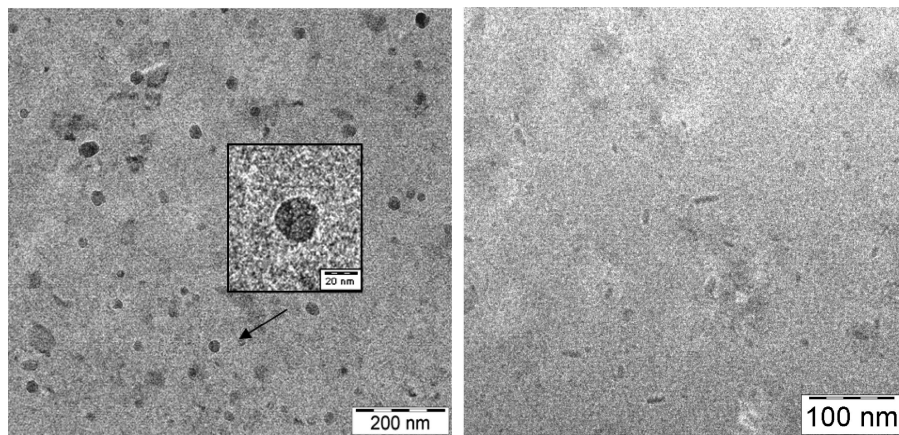


Figure 1. Cryo-TEM micrographs of polymer nanoparticles (left: Table 1, entry 7; right: entry 1).

infra) significantly reduce crystallinity of the high molecular weight polymers subject to this study by comparison to linear polyethylene. Via the catalyst precursor employed and the reaction conditions, a large range of crystallinities (as determined by DSC on the isolated bulk material, Table 1) and melting and crystallization temperatures is accessible. The overall branching observed for polymers prepared with catalysts based on the CF_3 -aryl-substituted ketoenamine (**1a,b**) is lower than for the isopropyl-substituted ketoenamine (**2b,c**), and higher polymerization temperatures favor branch formation due to increased β -H elimination, which is a key step in branch formation. For example, the polymer from entry 13 (catalyst precursor **2c**, 50 °C) has ca. 43 Me branches, 10 Et branches, and 10 C_{4+} branches per 1000 carbon atoms. By comparison, the polyethylene from entry 3 (catalyst precursor **1a**, 70 °C) has ca. 20 Me branches, 5 Et branches, and 1 C_{4+} branch per 1000 carbon atoms. Polymer obtained with the same catalyst precursor, but at a lower temperature (15 °C), has a considerably lower degree of branching (entry 2); only 7 Me branches were observed, and no higher branches were present according to ^{13}C NMR.

The shape and structure of the particles were studied by cryo-TEM (Figure 1 and Figure S11 in the Supporting Information). A thin film of a dispersion on a TEM grid was rapidly frozen by immersion in liquid ethane. The sample thus obtained, containing the polymer nanoparticles embedded in an amorphous ice matrix, was studied by TEM at -180 °C. The particles appear to be flat platelets with a polygonal circumference. This general structure is in agreement with a certain crystalline nature of the particles. In general, the particle sizes observed by TEM are in reasonable agreement with results of DLS (Table 1).¹⁵ Even after storing for more than a year at room temperature, the dispersions appeared unaltered as observed by cryo-TEM.

Summary and Conclusions

Despite the electron-deficient nature of the metal center, the water-soluble enolatoimine complexes studied are precursors to catalysts which are remarkably stable over time given the very high degree of dispersion of the aqueous polymerization system. Dispersions of particles of only 18 nm average size of polyethylene with substantial solids contents of up to 7 wt % are accessible. Via the substituents of the *N*-aryl moiety (2,6- $\text{R}_2\text{C}_6\text{H}_3$) and the polymerization temperature, the degree of branching of the polyethylenes generated in the form of very small (<30 nm) semicrystalline nanoparticles, and thus their crystallinity and melt transition temperatures can be varied over a wide range. In this study, nanoparticles of polymers with methyl and higher branches with a total branching ranging from 7 to 63 per 1000 carbon atoms, a T_m ranging from 75 to 129

°C, and (bulk) crystallinities from $\leq 25\%$ to 50% were prepared. Such dispersions of polyethylene nanoparticles in this size regime and with variable crystallinity are of interest for, among others, ultrathin films and nanocomposites.

Experimental Section

Materials and General Considerations. Unless noted otherwise, all manipulations of nickel complexes were carried out under an inert atmosphere using standard glovebox or Schlenk techniques. All glassware was flame-dried under vacuum before use. DMF and methanol- d_4 were thoroughly degassed by several freeze–pump–thaw cycles and stored in a nitrogen atmosphere glovebox. Benzene and benzene- d_6 was dried over sodium, vacuum transferred, and stored in a glovebox. Diethyl ether was distilled from purple sodium benzophenone ketyl under argon prior to use. Demineralized water was distilled under nitrogen and degassed three times after distillation. [(tmeda)NiMe₂] was supplied by MCAT (Konstanz, Germany). TPPTS was purchased from Aldrich and used as received. Me(OCH₂CH₂)_nNH₂ was purchased from Fluka and used as received (M_n = ca. 2320 g mol⁻¹). TPPDS was prepared according to ref 16. 1,1,1,5,5,5-Hexafluoro-2,4-pentanedione (99% purity) and 2,6-diisopropylaniline (90% purity, technical grade) were obtained from Acros. Sodium dodecyl sulfate (SDS) was purchased from Fluka. Ketoenamines were prepared according to published procedures.^{12b,c}

NMR spectra were recorded on a Varian Unity INOVA 400 or a Bruker Avance DRX 600 instrument. ^1H and ^{13}C NMR chemical shifts were referred to the solvent signal. High-temperature NMR measurements of polyethylenes were performed in 1,1,2,2-tetrachloroethane- d_2 at 130 °C in the presence of 0.5 wt % Cr(acac)₃ as a relaxation aid. Differential scanning calorimetry (DSC) was performed on a Netzsch Phoenix 204 F1 at a heating and cooling rate of 10 K min⁻¹. DSC data reported are from second heating cycles. Polymer crystallinities were calculated based on a melt enthalpy of 293 J g⁻¹ for 100% crystalline polyethylene. Gel permeation chromatography (GPC) was carried out in 1,2,4-trichlorobenzene at 160 °C at a flow rate of 1 mL min⁻¹ on a Polymer Laboratories 220 instrument equipped with Olexis columns with differential refractive index, viscosity, and light scattering (15° and 90°) detectors. Data reported were determined via linear PE standard calibration ($M_w < 3 \times 10^4$), universal calibration ($3 \times 10^4 < M_w < 10^5$), and triple detection ($M_w > 10^5$) employing the PL GPC-220 software algorithm. As the instrument records light scattering at only two angles, data analysis involves an iteration for the calculation of molecular weights and form factors for each measured interval. The instrument was calibrated with narrow polystyrene and polyethylene standards. Dynamic light scattering was carried out on a Malvern Nano Zeta Sizer. For the determination of particle size, a few drops of a latex sample were diluted with ca. 3 mL of water. Transmission electron microscopy was performed on a Zeiss Libra 120 EFTEM instrument, operated at

120 kV acceleration voltage. For cryo-TEM a Gatan cryo-transfer attachment CT3500 was used. For standard particle examination at room temperature one drop of the diluted dispersion was deposited on a carbon-coated 400 mesh copper grid and allowed to dry overnight. Specimens for cryo-TEM investigations were prepared in a Leica CPC instrument by freezing a thin film of the dispersion in liquid ethane. The thin film was created by dipping a small amount of the dispersion on a 1000 mesh grid. A meniscus, thin enough for TEM, forms over the holes in the grid and is rapidly frozen to afford a vitrified sample. The sample was then transferred cold into the TEM instrument and examined at a temperature around 90 K with minimal electron dose.

Synthesis and Characterization of Complexes. [κ^2 -N,O-3-[(2,6-Di(3,5-bis(trifluoromethyl)phenyl)phenyl)imine]methyl]-1,1,1,5,5,5-hexafluoro-pent-3-ene-2-one-4-olato]methyl(monoaminomonomethoxypoly(ethylene oxide))nickel(II) (**1a**). To a mixture of [(tmeda)NiMe₂] (20.4 mg, 100 μ mol) and ketoenamine (77.2 mg, 105 μ mol), benzene (4 mL) was added via syringe at 20 °C under a nitrogen atmosphere in a septum-capped Schlenk tube. Rapid reaction was evident from the immediate evolution of methane, which ceased within 5 min. The resulting red solution was stirred for 10 min at 20 °C, then a solution of Me(OCH₂CH₂)_nNH₂ (*M_n* = ca. 2320 g mol⁻¹, 200 mg, ca. 86 μ mol) in benzene (4 mL) was added by syringe, and the mixture was stirred for another 30 min. After sublimation of the frozen solvent (−5 °C) in vacuo, the residue was dispersed in diethyl ether (8 mL). The dispersed solid was collected by filtration and carefully washed with diethyl ether (3 × 5 mL). Removal of residual solvent under high vacuum (10⁻³ mbar) yielded **1a**.

¹H NMR (400 MHz, C₆D₆, 25 °C): δ /ppm = 7.98 (s, 4H, ortho CH of the CF₃-substituted aryl groups), 7.89 (s, 2H, para CH of the CF₃-substituted aryl), 7.49 (s, 1H, vinylic CH=C), 6.93–6.81 (br, 3H, C₆H₃), 3.6–3.2 (br, 214H, (CH₂CH₂O)_n), 3.13 (s, 3H, OCH₃), 3.05 (br, 2H, CH₂OCH₃), 2.13 (br, 2H, OCH₂CH₂NH₂), 1.28 (br, 2H, OCH₂CH₂NH₂), −1.02 (s, 3H, Ni–CH₃). ¹³C{¹H} NMR (100 MHz, C₆D₆, 25 °C): δ /ppm = 177.14 (q, ²J_{CF} = 32 Hz, CF₃CO), 169.54 (q, ²J_{CF} = 37 Hz, CF₃CO), 165.19 (imine C), 149.77 (C ipso to N), 141.28 (ipso C of the CF₃-substituted aryl groups), 133.13 (C ortho to N), 132.44 (q, ²J_{CF} = 33 Hz, meta C of CF₃-subst. aryl), 131.25 (C meta to N), 130.66 (ortho C of CF₃-substituted aryl), 127.37 (C para to N), 123.87 (q, ¹J_{CF} = 272 Hz, CF₃ bound to aryl), 121.44 (para C of CF₃-substituted aryl), 118.66 (q, ¹J_{CF} = 283 Hz, COCF₃), 116.94 (q, ¹J_{CF} = 291 Hz, COCF₃), 105.97 (vinylic C=CH), 70.99 ((CH₂CH₂O)_n), 58.65 (OCH₃), 42.16 (CH₂NH₂), −10.92 (Ni–CH₃). ¹⁹F NMR (376 MHz, C₆D₆, 25 °C): δ /ppm = −63.07 (aryl CF₃), −71.43 (CF₃CO), −73.08 (CF₃CO).

Sulfonated Phosphine Complexes. To a mixture of [(tmeda)NiMe₂] (20.4 mg, 100 μ mol) and ketoenamine (105 μ mol), DMF (2.0 mL) was added via syringe at 20 °C with stirring under a nitrogen atmosphere in a septum capped Schlenk tube. Rapid reaction was evident from the fast evolution of methane, which ceased within 5 min. The resulting red solution was stirred for 10 min at 20 °C. A DMF solution of TPPDS or TPPTS (95 μ mol in 1 mL of DMF) was added, and the mixture was stirred for another 30 min. The solvent was carefully removed under vacuum (10⁻³ mbar). The residue was suspended in diethyl ether (5 mL) and transferred to a gastight centrifugation vial. The suspension was repeatedly centrifuged, the supernatant was removed, and the residual dark red solid was redispersed with 5 mL portions of diethyl ether, until the supernatant remained colorless. Removal of residual solvent under high vacuum (10⁻³ mbar) yielded the corresponding complex.

[κ^2 -N,O-3-[(2,6-Di(3,5-bis(trifluoromethyl)phenyl)phenyl)imine]methyl]-1,1,1,5,5,5-hexafluoro-pent-3-ene-2-one-4-olato]methyl-[sodium di(p-sulfonatophenyl)phenylphosphine]nickel(II) (**1b**·2 DMF). ¹H NMR (400 MHz, CD₃OD, 25 °C): δ /ppm = 8.10 (s, 2H, para CH of the CF₃-substituted aryl), 8.08 (s, 4H, ortho CH of the CF₃-substituted aryl groups), 7.99–7.89 (m, 6H, vinylic CH=C, DMF, aryl H of C₆H₃), 7.82–7.72 (m, 4H, TPPDS), 7.40–7.30 (m, 6H, TPPDS), 7.30–7.22 (m, 3H, TPPDS), 2.94 and 2.80 (s each, 6H each, DMF), −1.21 (d, ³J_{PH} = 7.0 Hz, 3H, Ni–CH₃). ¹³C NMR (100 MHz, CD₃OD, 25 °C): δ /ppm = 178.1 (q, ²J_{CF} = 23

Hz, CF₃CO), 170.5 (q, ²J_{CF} = 29 Hz, CF₃CO), 166.7 (vinylic CH=C), 164.9 (br, DMF), 149.8 (ipso C of C₆H₃), 147.1 (br, TPPDS), 142.7 (ipso C of the CF₃-substituted aryl), 135.0 (d, ¹J_{CP} = 13 Hz, TPPDS), 134.6 (s, ortho C of C₆H₃), 134.5 (d, ¹J_{CP} = 13 Hz, TPPDS), 133.1 (q, ²J_{CF} = 34 Hz, meta C of CF₃-substituted aryl), 132.0 (ortho C of the CF₃-substituted aryl), 131.7 (meta C of C₆H₃), 130.45 (TPPDS), 129.9 (d, ¹J_{CP} = 6 Hz, TPPDS), 127.4 (para C of C₆H₃), 127.1 (d, ¹J_{CP} = 4 Hz, TPPDS), 124.9 (q, ¹J_{CF} = 181 Hz, CF₃), 124.8 (q, ¹J_{CF} = 180 Hz, CF₃), 122.6 (s, para C of the CF₃-substituted aryl), 116.00 (d, ¹J_{CP} = 15 Hz, TPPDS), 106.6 (vinylic C=CH), 37.0 and 31.7 (CH₃ each, DMF), −6.05 (d, ²J_{CP} = 23 Hz, Ni–CH₃). ¹⁹F NMR (376 MHz, CD₃OD, 25 °C): δ /ppm = −64.45 (aryl CF₃), −73.01 (CF₃CO), −74.36 (CF₃CO). ³¹P NMR (161 MHz, CD₃OD, 25 °C): δ /ppm = 33.06 (s).

[κ^2 -N,O-3-[(2,6-Diisopropylphenyl)imine]methyl]-1,1,1,5,5,5-hexafluoro-pent-3-ene-2-one-4-olato]methyl[sodium di(p-sulfonatophenyl)phenylphosphine]nickel(II) (**2b**·DMF). ¹H NMR (400 MHz, CD₃OD, 25 °C): δ /ppm = 7.93 (br, 2H, vinylic CH=C, DMF), 7.82 (br, 7H, TPPDS), 7.38 (br, 6 H, TPPDS), 7.15 (m, 3H, aryl), 3.68 (sept, ³J_{HH} = 6.5 Hz, 2H, CH(CH₃)₂), 2.94 and 2.80 (s each, 3H each, DMF), 1.34 (d, ³J_{HH} = 6.6 Hz, 6H, CH(CH₃)₂), 1.10 (d, ³J_{HH} = 6.2 Hz, 6H, CH(CH₃)₂), −1.24 (s, 3H, Ni–CH₃). ¹³C NMR (100 MHz, CD₃OD, 25 °C): δ /ppm = 178.7 (q, ²J_{CF} = 23 Hz, CF₃CO), 170.9 (q, ²J_{CF} = 25 Hz, CF₃CO), 164.9 (br, DMF), 162.5 (vinylic CH=C), 148.6 (ipso C of C₆H₃), 148.2 (br, TPPDS), 142.0 (ortho C of C₆H₃), 135.2 (d, ¹J_{CP} = 10 Hz, TPPDS), 135.4–134.4 (br, TPPDS), 129.8 (d, ¹J_{CP} = 7 Hz, TPPDS), 129.5 (CH, d, ¹J_{CP} = 9 Hz, TPPDS), 128.1 (para C of C₆H₃), 127.1 (CH, d, ¹J_{CP} = 6 Hz, TPPDS), 124.8 (meta C of C₆H₃), 119.3 (q, ¹J_{CF} = 188 Hz, CF₃), 118.0 (q, ¹J_{CF} = 193 Hz, CF₃), 116.00 (d, ¹J_{CP} = 15 Hz, TPPDS), 105.9 (vinylic C=CH), 37.0 and 31.6 (CH₃, DMF), 29.65 (CH(CH₃)₂), 25.00 and 23.27 (CH(CH₃)₂), −4.84 (br, Ni–CH₃). ¹⁹F NMR (376 MHz, CD₃OD, 25 °C): δ /ppm = −72.26 and −73.13 (CF₃CO). ³¹P NMR (161 MHz, CD₃OD, 25 °C): δ /ppm = 33.14 (s).

[κ^2 -N,O-3-[(2,6-Diisopropylphenyl)imine]methyl]-1,1,1,5,5,5-hexafluoro-pent-3-ene-2-one-4-olato]methyl[sodium tris(m-sulfonatophenyl)phosphine]nickel(II) (**2c**·DMF). ¹H NMR (400 MHz, CD₃OD, 25 °C): δ /ppm = 8.19 (br, 3H, TPPTS), 7.98 (s, 1H, vinylic CH=C), 7.93 (br, 2H, DMF), 7.87 (br, 3H, TPPTS), 7.55, 7.45, 7.34 (br each, 6H total, TPPTS), 7.14 (m, 3H, aryl), 3.66 (sept, ³J_{HH} = 6.5 Hz, 2H, CH(CH₃)₂), 2.93 and 2.80 (s each, 6H each, DMF), 1.36 and 1.11 (d, ³J_{HH} = 6.5 Hz, 6H each, CH(CH₃)₂), −1.20 (s, 3H, Ni–CH₃). ¹³C NMR (100 MHz, CD₃OD, 25 °C): δ /ppm = 178.6 (q, ²J_{CF} = 33 Hz, CF₃CO), 170.9 (q, ²J_{CF} = 36 Hz, CF₃CO), 165.1 (br, DMF), 162.5 (vinylic CH=C), 148.5 (ipso C of C₆H₃), 146.9 (br, TPPTS), 142.1 (ortho C of C₆H₃), 137.2 (br, TPPTS), 134.5 (d, ¹J_{CP} = 7 Hz, TPPTS), 131.84 (br, TPPTS), 129.8 (d, ¹J_{CP} = 6 Hz, TPPTS), 129.4 (br, TPPTS), 127.9 (para C of C₆H₃), 124.6 (meta C of C₆H₃), 119.1 (q, ¹J_{CF} = 285 Hz, CF₃), 118.0 (q, ¹J_{CF} = 291 Hz, CF₃), 105.75 (vinylic C=CH), 37.1 and 31.7 (CH₃, DMF), 29.56 (CH(CH₃)₂), 24.97 and 23.34 (CH(CH₃)₂), −4.46 (d, ²J_{CP} = 24 Hz, Ni–CH₃). ¹⁹F NMR (376 MHz, CD₃OD, 25 °C): δ /ppm = −72.08 and −73.06 (CF₃CO). ³¹P NMR (161 MHz, CD₃OD, 25 °C): δ /ppm = 35.03 (s).

Polymerization Procedure. Polymerizations were carried out in a 300 mL stainless steel mechanically stirred (750 rpm) pressure reactor equipped with a heating/cooling jacket supplied by a thermostat controlled by a thermocouple dipping into the polymerization mixture. A valve controlled by a pressure transducer allowed for applying and keeping up a constant ethylene pressure. The required flow of ethylene, corresponding to ethylene consumed by polymerization, was monitored by a mass flow meter and recorded digitally. Prior to a polymerization experiment, the reactor was heated under vacuum to the desired reaction temperature for 30–60 min and then backfilled with argon. To a mixture of SDS and the respective Ni–methyl complex 100 mL of distilled and degassed water were added at room temperature via a Teflon cannula in a 150 mL Schlenk flask. The mixture was stirred for 2 min to afford a homogeneous solution. The solution was cannula-transferred to the argon-flushed reactor, and the reactor was closed.

The reactor was pressurized to 40 bar with constant ethylene feeding under stirring. The final pressure was obtained within less than 3 min. After the desired reaction time, the reactor was carefully vented, and the obtained dispersion was filtrated through a plug of glass wool. For determination of yields and for further polymer analysis a specified portion of the dispersion was precipitated by pouring into excess methanol. The polymer was washed three times with methanol and dried in vacuo at 50 °C.

Acknowledgment. Financial support by the BMBF (project 03X5505) is gratefully acknowledged. We thank Marina Krumova for TEM and Lars Bolk for GPC analyses. S.M. is indebted to the Fonds der Chemischen Industrie and to the Hermann-Schnell Foundation.

Supporting Information Available: Figures showing GPC profiles, DSC and DLS traces, mass flow data for polymerization with **1a** and **2b**, ¹³C NMR spectra of polyethylenes, and additional cryo-TEM images of polymer particles. This material is available free of charge via the Internet at <http://pubs.acs.org>.

References and Notes

- (1) (a) Distler, D. *Wässrige Polymerdispersionen*; VCH: Weinheim, 1999. (b) Lovell, P. A.; El-Aasser, M. S. *Emulsion Polymerization and Emulsion Polymers*; Wiley: Chichester, UK, 1997. (c) Urban, D.; Takamura, K. *Polymer Dispersions and their Industrial Applications*; Wiley-VCH: Weinheim, 2002. (d) *Chemistry and Technology of Emulsion Polymerisation*; Van Herk, A., Ed.; Blackwell Publishing Ltd: Oxford, UK, 2005. (e) Charleux, B.; Ganachaud, F. Polymerization in Aqueous Dispersed Media. In *Macromolecular Engineering*; Matyjaszewski, K.; Gnanou, Y.; Leibler, L., Eds.; Wiley-VCH: Weinheim, 2007; Vol. 1, pp 605–642.
- (2) (a) Caruso, F. *Colloids and Colloid Assemblies*; Wiley-VCH: Weinheim, 2004. (b) Haag, R. *Angew. Chem.* **2004**, *116*, 280–284. (c) Haag, R. *Angew. Chem., Int. Ed.* **2004**, *43*, 278–282. (d) Bosman, A. W.; Janssen, H. M.; Meijer, E. W. *Chem. Rev.* **1999**, *99*, 1665–1688. (e) Grayson, S. M.; Fréchet, J. M. J. *Chem. Rev.* **2001**, *101*, 3819–3868. (f) Cölfen, H. *Macromol. Rapid Commun.* **2001**, *22*, 219–252. (g) Allen, T. M.; Cullis, P. R. *Science* **2004**, *303*, 1818–1822. (h) Broz, P.; Driamov, S.; Ziegler, J.; Ben-Haim, N.; Marsch, S.; Meier, W.; Hunziker, P. *Nano Lett.* **2006**, *6*, 2349–2353. (i) Kunna, K.; Müller, C.; Loos, J.; Vogt, D. *Angew. Chem., Int. Ed.* **2006**, *45*, 7289–7292.
- (3) (a) Kuo, P. L.; Turro, N. J.; Tseng, C. M.; El-Aasser, M. S.; Vanderhoff, J. W. *Macromolecules* **1987**, *20*, 1216–1221. (b) Feng, L.; Ng, K. Y. S. *Macromolecules* **1990**, *23*, 1048–1053. (c) Ferrick, M. R.; Murtagh, J.; Thomas, J. K. *Macromolecules* **1989**, *22*, 1515–1517. (d) Perez-Luna, V. H.; Puig, J. E.; Castano, V. M.; Rodriguez, B. E.; Murthy, A. K.; Kaler, E. W. *Langmuir* **1990**, *6*, 1040–1044. (e) Antonietti, M.; Basten, R.; Lohmann, S. *Macromol. Chem. Phys.* **1995**, *196*, 441–466. (f) Pavel, F. M. *J. Dispersion Sci. Technol.* **2004**, *25*, 1. (g) Capek, I.; Juranicová, V.; Barton, J.; Asua, J. M.; Ito, K. *Polym. Int.* **1997**, *43*, 1–7. (h) Loh, S.-E.; Gan, L.-M.; Chew, C.-H.; Ng, S.-C. *J. Macromol. Sci., Pure Appl. Chem.* **1995**, *32*, 1681–1697.
- (4) (a) Sommer, J.; Reiter, G. *Adv. Polym. Sci.* **2006**, *200*, 1–36. (b) Reiter, G.; Castelein, G.; Sommer, J.-U.; Röttele, A.; Thurn-Albrecht, T. *Phys. Rev. Lett.* **2001**, *87*, 226101–1 to –4. (c) Montenegro, R.; Antonietti, M.; Mastai, Y.; Landfester, K. *J. Phys. Chem. B* **2003**, *107*, 5088–5094.
- (5) (a) Tong, Q.; Krumova, M.; Mecking, S. *Angew. Chem., Int. Ed.* **2008**, *47*, 4509–4511. (b) Tong, Q.; Krumova, M.; Göttker-Schnetmann, I.; Mecking, S. *Langmuir* **2008**, *24*, 2341–2347.
- (6) Strobl, G. R. *The Physics of Polymers*, 3rd ed.; Springer: Berlin, 2007.
- (7) Weber, C. H. M.; Chiche, A.; Krausch, G.; Rosenfeldt, S.; Ballauff, M.; Harnau, L.; Göttker-Schnetmann, I.; Tong, Q.; Mecking, S. *Nano Lett.* **2007**, *7*, 2024–2029.
- (8) Kolb, L.; Monteil, V.; Thomann, R.; Mecking, S. *Angew. Chem., Int. Ed.* **2005**, *44*, 429–432.
- (9) Göttker-Schnetmann, I.; Korthals, B.; Mecking, S. *J. Am. Chem. Soc.* **2006**, *128*, 7708–7709.
- (10) (a) Zuideveld, M.; Wehrmann, P.; Röhr, C.; Mecking, S. *Angew. Chem., Int. Ed.* **2004**, *43*, 869–873. (b) Göttker-Schnetmann, I.; Wehrmann, P.; Röhr, C.; Mecking, S. *Organometallics* **2007**, *26*, 2348–2362. (c) Bastero, A.; Göttker-Schnetmann, I.; Röhr, C.; Mecking, S. *Adv. Synth. Catal.* **2007**, *349*, 2307–2316.
- (11) Decomposition and polymerization mechanisms: (a) Berkefeld, A.; Mecking, S. *J. Am. Chem. Soc.* **2009**, *131*, 1565–1574. (b) Jenkins, J. C.; Brookhart, M. *J. Am. Chem. Soc.* **2004**, *126*, 5827–5842.
- (12) (a) Wang, C.; Friedrich, S.; Younkin, T. R.; Li, R. T.; Grubbs, R. H.; Bansleben, D. A.; Day, M. W. *Organometallics* **1998**, *17*, 3149–3151. (b) Zhang, L.; Brookhart, M.; White, P. S. *Organometallics* **2006**, *25*, 1868–1874. (c) Yu, S.-M.; Berkefeld, A.; Göttker-Schnetmann, I.; Müller, G.; Mecking, S. *Macromolecules* **2007**, *40*, 421–428.
- (13) Connor, E. F.; Younkin, T. R.; Henderson, J. I.; Waltman, A. W.; Grubbs, R. H. *Chem. Commun.* **2003**, 2272–2273.
- (14) (a) Randall, J. C. *J. Macromol. Sci., Rev. Macromol. Chem. Phys.* **1989**, *C29*, 201–317. (b) Axelson, D. E.; Levy, G. C.; Mandelkern, L. *Macromolecules* **1979**, *12*, 41–52.
- (15) For some samples containing larger particles, a discrepancy between TEM and DLS was observed (e.g., entry 1; DLS: 105 nm; cryo-TEM: 30 nm). This might be due to the formation of aggregates in solution at the variable concentrations of the two different analysis methods.
- (16) Herd, O.; Hessler, A.; Langhans, K. P.; Stelzer, O.; Sheldrick, W. S.; Weferling, N. *J. Organomet. Chem.* **1994**, *475*, 99–111.

MA9003665